Glass poling as a substrate surface pre-treatment for *in situ* metal nanoparticle formation by reduction of metal salt

TamilSelvi Selvam[1], Petar Pervan[1], Jordi Sancho-Parramon[1], Maria Chiara Spadaro[2], Jordi Arbiol[2,3], Vesna Janicki[1]*

[1]Ruđer Bošković Institute, Bijenička c. 54, 10000 Zagreb, Croatia

[2]Catalan Institute of Nanoscience and Nanotechnology (ICN2), CSIC and BIST, Campus UAB, Bellaterra, 08193 Barcelona, Catalonia, Spain

[3]ICREA, Pg. LluísCompanys 23, 08010 Barcelona, Catalonia, Spain

*corresponding author: janicki@irb.hr

Abstract

Metal nanoparticles are used in optical coatings and sensors due to their absorption in optical part of spectrum and its sensitivity to the environment induced by localized surface plasmon resonance. Glass is the most common substrate used for optical coatings. However, its surface does not have optimal properties for coating with metal nanoparticles grown *in situ* by reduction of metal salt. Glass surface optimization methods may involve environmentally hostile chemicals or processes that have time limited or atmosphere sensitive effects. In this study it is demonstrated and discussed effectiveness, mechanisms and advantages of glass poling as pre-treatment method for improving glass surface properties for maximization of coatings plasmonic performance. Pre-treatment of glass surfaces by poling is highly efficient for the purpose. Glass poling quenches ion exchange between metal ions from the solution and alkali ions from glass, favouring nanoparticles formation. Surface prepared in such way is not affected by ageing in normal atmosphere and is effective even after coating with ultrathin dielectric or Cr layers.

Keywords: metal nanoparticles, thin films, optical properties, glass poling, surface modification, ion exchange

1. Introduction

Metal nanoparticles (MNPs) have interesting optical properties that are dominated by localized surface plasmon resonance (LSPR) responsible for strong absorption at relatively narrow range of optical wavelengths [1]. MNPs in thin films are used for sensors [2], absorbers [3], reflectors [4] among others. For many applications it is beneficial to have high intensity of LSPR peak. Its intensity is related with concentration, size and size distribution of MNPs. Thin films containing MNPs can be fabricated by different techniques, such as physical vapour deposition or spin coating of solution containing metal salts followed by annealing [5]. In the last case, absorptance of the coating is limited by the maximal attainable metal salt concentration in the solution and by the coating thickness that can be realized. The thickness depends on the samples surface susceptibility to bond MNPs or the solution, among other reasons.

The material most frequently used for optical purposes is glass. Glass is widely available material, optically transparent, mechanically and chemically stable. For these reasons it is a typical choice as a material for optical coatings substrates. Common glasses consist mainly of silica, alkali and alkali earth (such as Na, K, Ca or Mg) compounds, which content may easily reach 30% or more. The most common are soda-lime glasses. However, coating glass surface with different solvents containing MNPs or dissolved metal salts is not always easy because of poor wetting or very weak attachment of MNPs. Therefore, very often glass surface first has to be properly prepared. Some of the methods for improving glass surface properties that are important for wet chemistry methods are plasma cleaning or chemical surface functionalization [6,7]. Chemicals that are used for this purpose are not always environmentally friendly.

Glass poling (GP) enables compositional, optical and surface modifications of glass and can be applied to alkali or alkali earth containing glasses. Ideal case of silica matrix is crystalline quartz where silica molecules are bonded to each other by bridging oxygen bonds, forming tetrahedrons [8]. However, glass matrix contains significant concentration of non-bridging oxygen bonds [9]. Their electronegativity is neutralized by alkali or alkali earth ions that are nesting in their vicinity. During glass poling mobility of ions increases as glass is warmed up and the applied external electric field directs ions drift towards cathode. Hydronium ions (H_3O^+, positive charge carriers) from glass surface and air partially compensate lack of positive charge in depleted region. Since hydrogen supply from the surface and atmosphere in

normal conditions, i.e. with anode pressed on the substrates surface, is insufficient for complete charge compensation, also non bridging oxygen bonds transform into bridging ones with release of oxygen [8, 10]. As a consequence of uncompensated charge, a zone permanently depleted from alkali and alkali earth ions and permanent internal electric field is created in the glass subanodic region [11]. Due to the change in composition, the value of refractive index in depleted zone is closer to the value for pure silica [12-14]. Besides this, volume of the depleted region shrinks (relaxes) [15] and the surface changes its hydrophilicity, depending on the kind of glass [16-19]. The depleted region is maintained until glass is heated close to its transition temperature [20]. Selectively poled glass surfaces can be used for microstructuring with MNPs, not only by immersion of poled glass into salt melt [21, 22], but also using spin coating and *in situ* MNPs growth by the reduction of metal salt as well [23].

Following the work in the last mentioned reference, in this study we propose GP as a new, simple and clean method for improvement of glass susceptibility for efficient coating with MNPs grown *in situ* and discuss possible mechanisms. The improved susceptibility does not deteriorate with surface exposure to normal atmosphere and it is effective in thin multilayer systems as well.

1. Materials and Methods

For the experiments 1 mm thick Menzel microscope slides were used (in further text also referred as soda-lime glass). It is a typical soda-lime glass containing nearly one fourth of alkalis and alkali earth oxides, mainly sodium oxide. Also 1 mm thick Schott KF9, BK7 and UV grade quartz glasses were used (for glasses composition see Supplement information). The substrates were cleaned, poled, coated, annealed and finally analysed.

Prior to glass poling, the substrates were wiped with acetone and ethanol, dried with cotton and finally puffed with nitrogen. A glass slab coated with Cr was used as an anode (Fig. 1). One part of the substrate was masked prior to Cr deposition, so after coating a bare glass window was obtained in the conductive Cr layer. In this way it was possible to carry out locally selective GP: no electrical contact beneath the window means no poling and the properties in this part of the sample remain unchanged. The non-poled part of the sample will be referred as step since it makes a physical step at the surface due to the volume relaxation of the poled part [15]. The standard poling conditions applied in this study were $300^{o}C$ and $500V$ for 1 h.
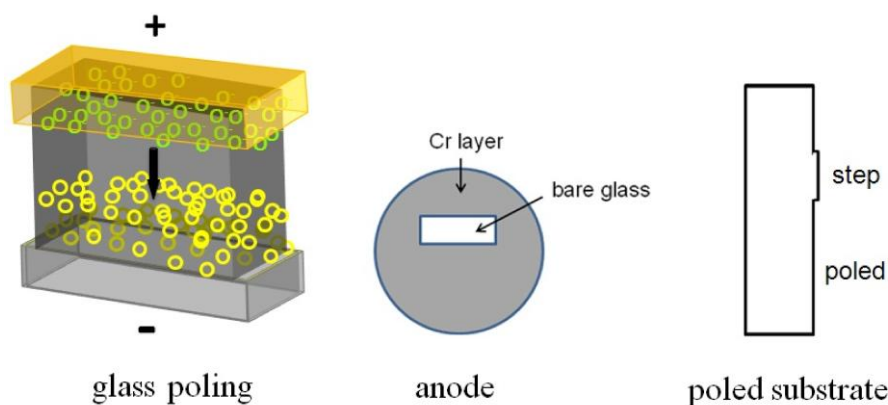
Fig. 1. Scheme of the used anode, glass poling set-up (yellow circles - alkali ions, green circles H^+/H_3O^+) and the resulting substrate. The obtained step height for soda-lime glass after the standard GP is approx. 80 nm.

Coating solution was prepared as 0.1 M of silver nitrate ($AgNO_3$) in acetonitrile and 3% polyvinylpirrolydone (PVP) also in acetonitrile, in equal volumes. Spin coating was done in dynamic mode. As a standard procedure, the substrates were coated one day after GP. Afterwards, the substrates were annealed in air at 200 ^{o}C for 20 minutes to enable formation of Ag NPs.

The samples optical properties were analysed from spectrophotometric and ellipsometric measurements, both performed with J.A. Woollam V-VASE ellipsometer. Ellipsometric Ψ and Δ functions were measured under 45°, 55° and 65° angle of incidence in spectral range 0.57 - 3.8 eV (corresponding to 2175 - 326 nm). Transmittance (T) was measured by the same device, at normal incidence. Characterisation of samples optical properties was based on ellipsometric measurements and performed using WVASE32 software.

Particles distribution on samples surface and its composition were checked by scanning electron microscopy (SEM), energy-dispersive x-ray spectroscopy (EDS) and scanning transmission electron microscopy - electron energy loss spectroscopy (STEM-EELS). In particular STEM-EELS has been acquired on a field emission gun (FEG) FEI Tecnai F20 microscope coupled to aGATAN QUANTUM filter.

2. Results and discussion

Glass poling and spin coating with the applied solution do not change visual appearance of the samples in the sense that they remain transparent and colourless. The appearance changes

upon Ag NPs formation during annealing. Clear difference between step and poled region upon annealing is obtained. Poled region presents more intense yellow coloration in transmittance than the step one (Fig. 2, inset), appearing like there is more Ag NPs in the coating over poled than step region. This means that the glass surface becomes sensitive to the formation of Ag NPs after poling.

Transmittance spectra of both regions (Fig. 2) have a dip around 2.8 eV that corresponds to absorption of Ag NPs, resulting in yellow coloration of transmitted light. Transmittance intensity difference of the two regions at this energy is approximately 25%, poled being the lower one. Ellipsometric functions present clear difference between the two regions as well (Supplement information).
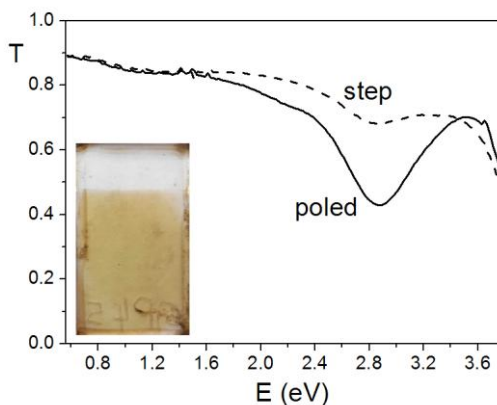

Fig. 2. Transmittance spectra of poled and step region. Inset: coated poled soda-lime substrate after annealing. White stripe presents step and yellow is poled region.

For better understanding of ellipsometric functions graphs it is useful to compare Ψ spectra of virgin and uncoated poled glass (Fig. 3). One may notice that Ψ of virgin glass, corresponding to uncoated step region, is basically a flat line, while the poled glass curve has fringes that resemble to thin films interference fringes in reflectance or transmittance. Indeed, the fringes are a fingerprint of the depleted region presenting lower refractive index than bulk glass, thus acting as a thin film over the glass surface. The fringes can be noticed in transmittance measurements of the same sample as well (not presented here). Regarding the coated samples, Ψ of the step region resembles the one of untreated bare glass (virgin), except around 2.8 eV where it forms plasmon peak. Ψ of poled part presents the fringes originating from the depleted region and peak originating from plasmon resonance that is much more intense than for the step region. It is important to notice that poled glass subanodic refractive index profile

($n(d)$) has to be taken into account in the course of optical characterization of the coated poled region: on Fig. 3b) glass surface is positioned at 0 nm, negative part of d axes represents distance from glass surface towards bulk. Depleted region, formed within the first 200 nm from the surface, is followed by refractive index peak originating from piled up alkali earth ions [14].
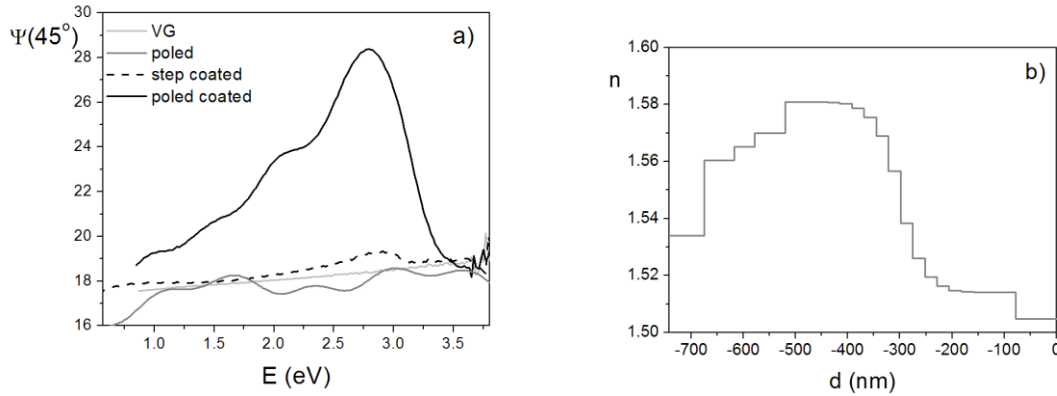

Fig. 3. Comparison of Ψ spectra originating from GP and LSPR for different samples: uncoated bare glass (VG), uncoated poled and coated poled and step region (a). For clarity, only measurements at 45° are presented. Refractive index profile of poled uncoated soda-lime glass at 2.48 eV (b).

In the course of optical characterization the coating was modelled using multiple Gaussian oscillators to take into account the LSPR of Ag NPs in PVP [24]. Optical characterisation results for layers thickness (d), $n(d)$ and imaginary part of the dielectric function (ε_2), describing plasmon peak (LSPR), are presented in Fig. 4. Coating with Ag NPs and PVP is presented at positive side of d axes. The coatings thicknesses are approximately 50 nm. Same as T dips of the two regions (Fig. 2), plasmon peaks confirm that absorption is stronger at poled region (Fig. 4 b)). Peak positions are located at the same energy. Poled region ε_2 peak has nearly 6 times higher intensity. Since the layers thickness over both regions is nearly the same and plasmon peak is weaker for the step, it is suggested that there are less NPs in the layer covering step than the poled region. Assuming the distance between NPs is long enough so there is no electromagnetic coupling among them, the ratio of extinction coefficients or ε_2 is proportional to the ratio of NPs concentration of the two regions [25]. Thus, it is estimated that there are nearly 6 times more particles per unit of thickness in poled than in step region of the coating. SEM micrographs confirm more NPs at the surface of poled region (Fig. 5).
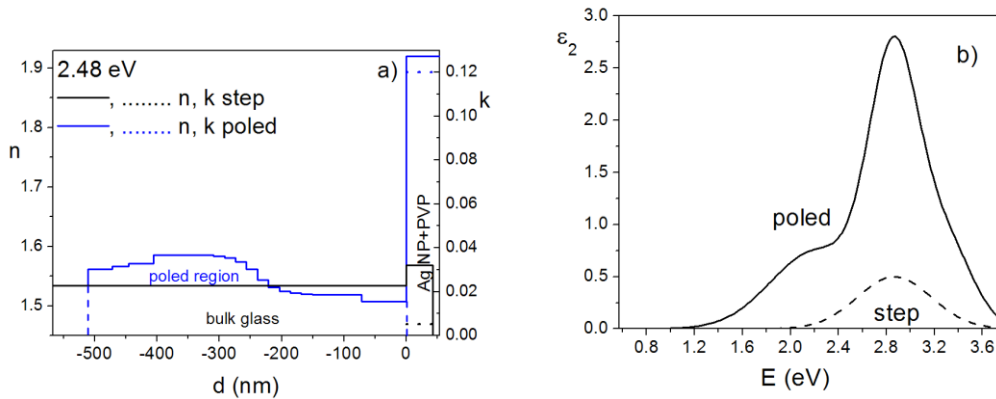
6

Fig. 4. Refractive index profile of the coated step and poled region (a) and dielectric function imaginary parts of the two regions (b).
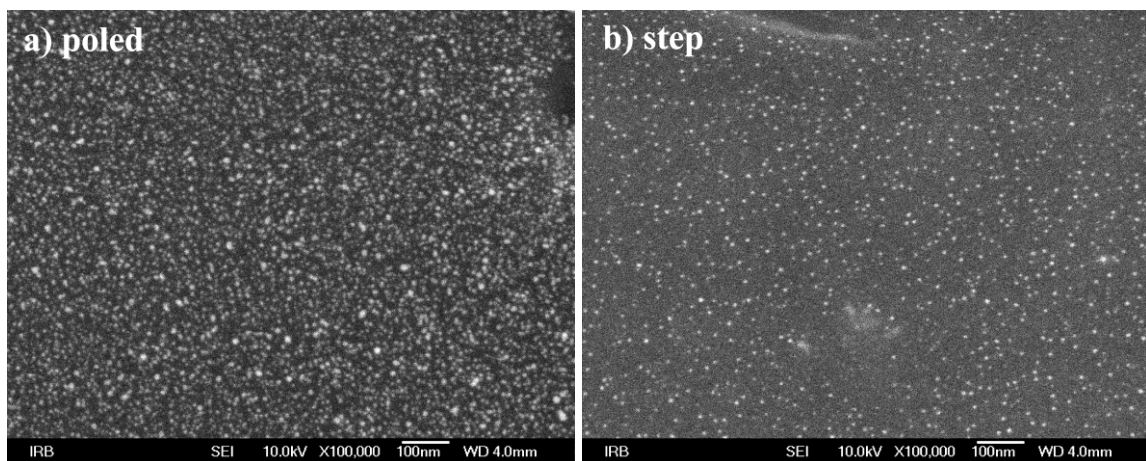

Fig. 5. SEM micrographs of the coated poled (a) and step (b) region.

In addition to Ag NP, it is demonstrated that better susceptibility for formation of NPs is valid for the case of Au NP as well. The resulting ε_2 confirms again lower plasmon intensity at step region. However, the difference between the two is not so pronounced as in the case of Ag containing sample. The obtained SEM micrographs (see Supplement information) again present higher NPs density at poled region, but these at step are bigger.

The question of what is the origin of this effect arises. Generally, there are many parameters that have impact to optical properties of spin-coated layers. Possible mechanisms that should be considered are that a) GP removes impurities that are adhered at glass in somewhat similar way that plasma cleaning does, so more solution may remain at the surface, b) GP changes hydrophilicity or surface roughness and again more liquid may remain after spinning, c) GP

forms alkali depleted subanodic region that prevents ion exchange (IE) among alkalis from glass and Ag from the coating, and finally d) H^+/H_3O^+ enriched poled region surface prevents diffusion of Ag^+ into glass. Additional experiments had to reveal which of the possible mechanisms is dominant.

3.1. Surface quality influence

One of standard procedures to remove impurities from glass surface is plasma cleaning (PC). However, impurities attach back soon after the exposure of the surface to the atmosphere. In this sense, if GP has a similar role, longer time between poling and coating might lead to the lower ε_2 contrast of the two regions. Therefore, different times were let to pass between poling and coating, ranging from 45 minutes to one week. For samples poled within one day after poling no significant change that could be ascribed to the longer exposition of poled glass to the normal atmosphere alone was noticed (Fig. 6). Interestingly, contrary to the expectations, poled region of the sample coated after one week presents somewhat stronger intensity around LSPR energy.

Standard poling time of 1 h was applied in this study for the sake of easier control of poling efficiency by fringe appearance. However, appearance of fringes related to the existence of depleted region may be unwanted for some applications. It is important to notice that reduction of depleted region thickness with reduction of poling time is favourable for fringes suppression. Indeed, the treatment time can be shorter as 30 minutes of poling is demonstrated to be equally effective for Ag NPs formation, as presented in Fig. 6.
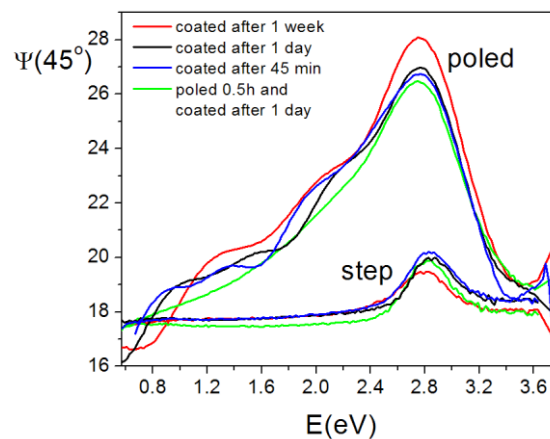
Fig. 6. Experimental Ψ function for samples with poling to coating time between 45 min and 1 week and for the sample poled for 30 min. For clarity, only measurements for 45° are presented. Note nearly complete absence of fringes due to the reduced poling time.

In order to compare the effects of GP and surface cleaning, one soda-lime substrate was subjected to PC (Ar, 6 keV, 2 minutes) upon GP and prior to coating. Comparing the two regions (step: PC prior to coating, poled: GP and PC prior to coating), the poled one shows again significantly stronger coloration (see Supplement information). Also, more intense yellowish coloration appears at step region of this sample than at step of a standard one. This confirms that for obtaining intense plasmon on glass surface GP is more effective than PC.

3.2. Hydrophilicity influence

As mentioned before, poling changes hydrophilicity of glass: in the case of glass with high boron content hydrophilicity is higher after poling [16, 17] and in the case of soda-lime glass it is lower [18, 19]. In order to suppress the possible influence of change of hydrophilicity upon GP, thin layers of 10 nm of SiO_2 or 2 nm, 5 nm and 10 nm of TiO_2 were evaporated to poled substrates before spin coating. Substrate coated with 4 nm of Cr followed by 7 nm of SiO_2 was prepared as well. These layers were deposited using electron beam evaporation onto the unheated substrates. TiO_2 was deposited in reactive oxygen atmosphere. Prior to the deposition, longer half of the substrate was masked with tape. Thus, only one half of each region (poled and step) was coated with dielectric. This enabled direct comparison of differently treated regions on the same sample. As a result, step region had again significantly higher transmittance than the poled one (Fig. 7).
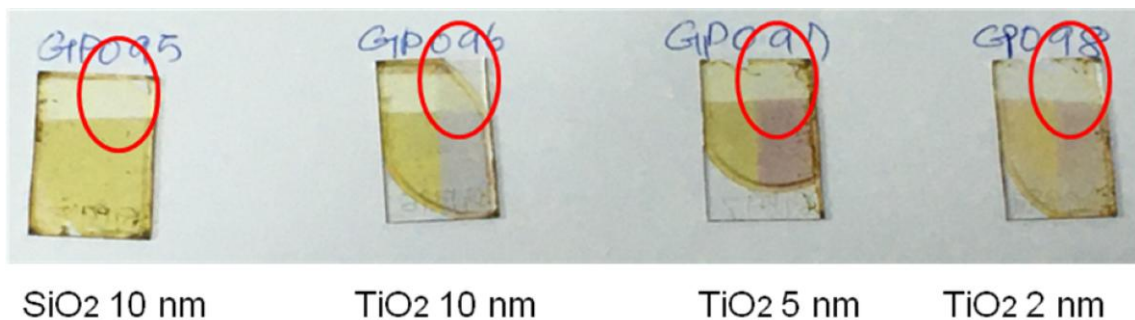

Fig. 7. Poled substrates coated with thin dielectric layer prior to spin coating (right half of each sample). The upper part of each substrate (stripe) presents step and the lower poled region. The difference of transmittances between the two regions is significant despite thin

dielectric layer between substrate and Ag NP coating (red ellipses). Difference in coloration for TiO_2 coated samples originates dominantly from interference.

Transmittance and ellipsometric functions of Cr containing sample are influenced by absorption at both, Cr layer and Ag NPs. Therefore, it was necessary to make optical characterization and reveal Ag plasmon ε_2 only, to compare nanoparticles containing coating with the previous samples. The obtained results again present poled region ε_2 intensity significantly higher than for step region (Supplement information).

It should be noted at this point that dielectric or Cr layers deposited onto the poled sample should mask the possible differences in roughness, or hydronium ions presence of the two regions as well.

Generally, cleaner surface, higher hydrophilicity or roughness of the poled region, would result in a thicker coating. Modelling shows that thickness over poled region should be six times higher than over step region in order to explain so high contrast of transmittance. This is not supported with the results from optical characterization: as seen from Fig. 4 the coating over poled region is thicker than the one over step region less than 20%. One has to keep in mind that step region is placed away from the centre of rotation during spin coating (Fig. 2 inset, Fig. 7), while the measurements of poled region were always made in the centre. Depending on the viscosity and spinning parameters, it is possible that the coating has certain thickness nonuniformity, i.e., that thickness decreases with distance from the centre of rotation [26]. Indeed, comparing coating thicknesses obtained from measurement in the centre and edge of a test coated virgin glass sample, the first one is 9 nm thicker than the later one, which is in accordance with data from Fig. 4.

3.3. Ion exchange among glass and the coating

The next hypothesis that could explain higher susceptibility for formation of Ag NPs on poled glass is that above the step region Na ions from the glass exchange with Ag ions from the coating [27-29]. This could result in lower concentration of Ag ions forming NPs in the coating later. Contrary to this, poled region is depleted from Na, so IE with coating above is practically prohibited.

Dielectric layers evaporated by electron beam, as in experiments described previously in this study, are not necessarily effective barrier to IE. A way to exclude or reduce ion exchange in the experiments is to use substrates without or with lower alkali content than in Menzel glass.

Appropriate substrates, quartz and BK7 glass, were treated in the same manner as the previous standard samples. For comparison, the same test was done also with KF9 glass, having higher Na content than soda-lime. Fig. 8 shows no difference among poled region plasmon peak intensities for diverse glasses. On the other hand, step region plasmon peak clearly decreases with increasing alkali content. There is no difference in plasmon for poled and step region in the case of quartz. Plasmon peak at BK7 is lower, while the intensities at KF9 and Menzel are the lowest and nearly equal. Conclusion is that higher concentration of alkalis enables more Ag ions to diffuse into glass. Ag remains in ionic state in glass matrix upon diffusion because annealing temperature is too low to enable formation of NPs. Although present in the sample, ionic Ag does not contribute to the plasmon intensity. The remaining Ag ions in the coating form NPs giving weak plasmonic response of the coating, such is the case of coatings at KF9 and Menzel glass.
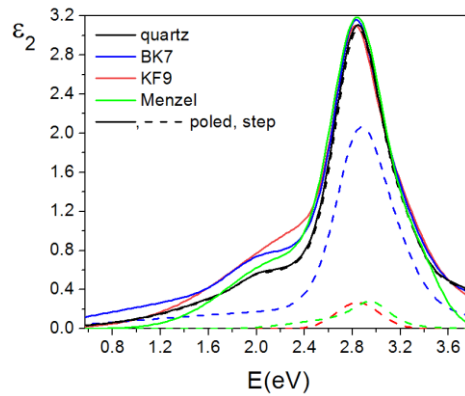

Fig. 8. Plasmon intensity at step and poled region for different types of substrates.

Results from the set of the samples prepared with higher $AgNO_3$ concentrations (0.2 M and 0.3 M of $AgNO_3$ in acetonitrile and 6% and 9% of PVP also in acetonitrile, in equal volumes) [23] are in accordance with ion exchange explanation. Fig. 9 shows that the two regions ε_2 difference decreases as $AgNO_3$ concentration increases. This may be a consequence of alien ion concentration saturation in the substrate and the coating, i.e. reaching maximum concentration of Ag^+ in glass and Na^+ in the coating, for given ion exchange conditions. The coated samples were measured again after three months and no difference in ε_2 indicating continuation of the process was found.
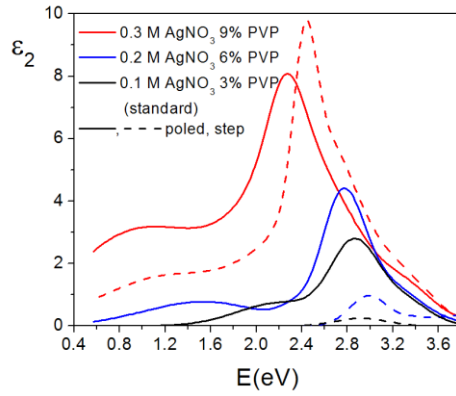
Fig. 9. Poled and step region ε_2 for different concentrations of AgNO$_3$

Searching for confirmation of Na$^+$ and Ag$^+$ IE between glass and coating, the standard samples were examined by SEM and EDS. Regular shape grains at step region are visible on SEM micrographs. These crystallites are bigger and denser at the sample with higher Ag concentration (0.3 M AgNO$_3$ and 9% PVP) (Fig. 10 a), b)). The grains were not found at poled region. Much higher EDS Na signal at crystallite site (see Supplement information), relative to Mg and Ca signals from background (substrate), is clear evidence of out diffusion of Na from glass.
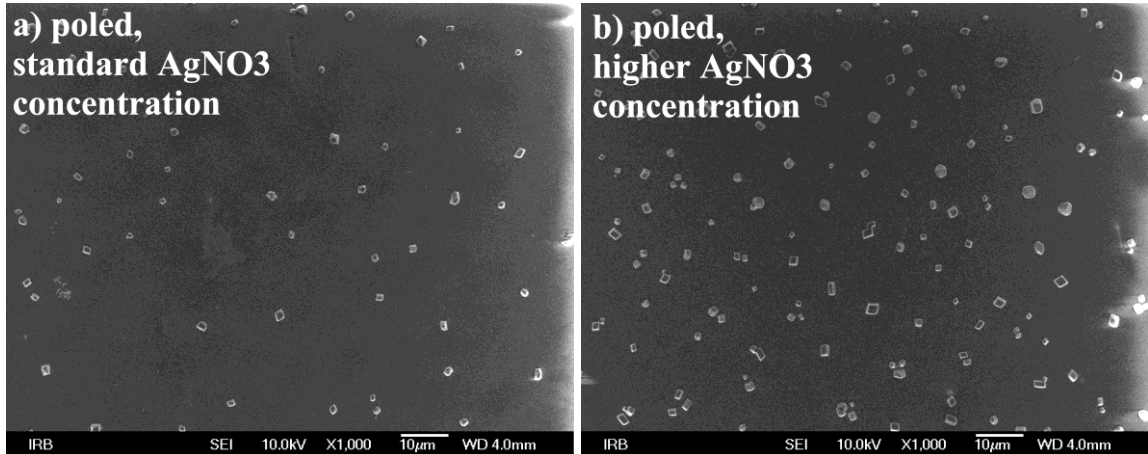

Fig. 10. SEM micrographs: step region standard sample (a) and the one with higher Ag concentration in the coating (b).

Additional EDS analysis was performed for standard sample before and after coatings removal (Table 1. and Fig. 11, respectively). It confirms that the coating over poled region has higher content of Ag than over step and no Na, as expected.

Due to its lower mobility than Na and Ca ions, Mg remains closer to the surface upon poling [14] and therefore appears in EDS of the poled region. Glass surface EDS analysis made after coating was removed by cotton and ethanol, presents only traces of Mg in poled region (Fig. 11 a)). Step region (Fig. 11 b)), besides alkalis, evidences Ag that remains in glass subsurface region explained as a consequence of IE.

Table 1. Composition of coated poled and step surface from EDS measurements.

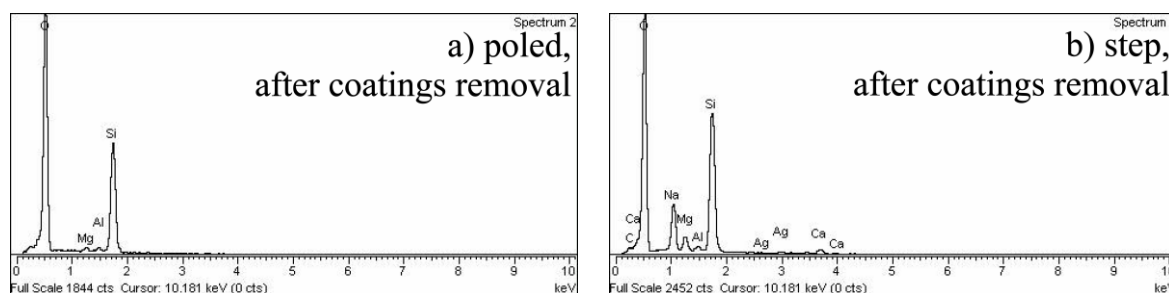| w% / region	Ag	Na	Ca	Mg	C	O	Al	Si
step	0.11	3.94	0.05	0.75	28.41	62.02	0.13	4.60
poled	0.49	-	-	0.21	25.39	66.11	0.21	7.58

Fig. 11. EDS of glass surface after removal of the coating: poled (a) and step region (b).

It can be concluded that *in situ* growth of NPs by the reduction of metal salt in the coating involves unwanted ion exchange between virgin substrate and the coating, resulting in loss of plasmon intensity. Ag^+ from the coating is exchanged by Na^+ from glass (the most mobile alkali in the glass) providing less metal ions in the coating. Upon GP, the subsurface region is depleted from alkali ions and IE is prevented. Therefore, the coated layer remains Ag^+ rich and able to form higher concentration of NPs resulting in more intense LSPR peak. As demonstrated, GP is effective also in the case of Au NPs, since Au^+ are participating in IE, though in lesser extent than Ag^+ due to their lower mobility [30].

3.4. Role of H^+/H_3O^+

As mentioned before, GP surface is enriched with H^+/H_3O^+. When poling is done in vacuum or with anodic layer deposited onto glass, the enrichment is substantially lower [8, 31]. In order to check hydronium role in formation of Ag NPs in the coating, two substrates were

poled in vacuum, under standard conditions. One of them was coated after it was exposed to atmosphere for two days and the other immediately (within one hour) upon exposure to normal atmosphere. The visual appearance upon annealing of the first one was like for the previous samples, with clear distinction of the step (faintly coloured) and poled (intensive coloured) region. However, both regions of the second sample were faintly coloured, without clear boundary between them.

In accordance with this, the appearance of LSPR intensities of the first sample are the same as for the samples made in the standard way, i.e. step and poled ε_2 peak intensity, is clearly higher for poled then step region. The second sample poled region ellipsometric measurements present characteristic fringes evidencing existence of depleted sublayer (Supplement information). However, ε_2 peaks do not differ significantly in the step and poled region (Fig. 12). Their intensity and shape correspond to ε_2 of standard sample step region. This indicates lack of Ag in coating over both, step and poled region suggesting that Ag has diffused into glass regardless to poling.
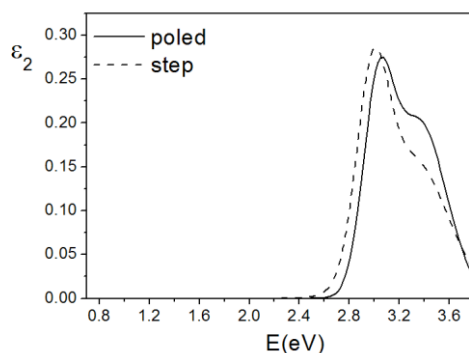

Fig. 12. The sample coated immediately after poling in vacuum: comparison of ε_2 for step and poled region.

This is in accordance with another study where is shown that Ag^+ from hot salt melt bath enter into vacuum poled glass and form NPs there [32]. In our case NPs in glass were not observed after coating removal. Reason for this may be much lower concentration of Ag in the solution than in the melt.

Detailed cross-section analysis was made by STEM-EELS for the sample poled with standard GP conditions in air and coated after 45 min (Fig. 13). The coating was removed before the examination. Step region analysis shows a thin layer (approx. 10 nm) rich in Na at the samples surface, which is in accordance with IE. Ag penetrated relatively deep into glass. It is

distributed quite uniformly within the analysed depth, having somewhat higher concentration near the surface. Regarding poled region, the analysed depth corresponds to the depletion region depth (Fig. 4. a)): Na concentration is low and constant. The first 300 nm from the surface is free of Ag; it is accumulated deeper in the sample. Comparing with Fig 4.a), the depth where Ag collected corresponds to $n(d)$ peak position, formed due to alkali earth ions (Ca^{2+} and Mg^{2+}) pile up in the space charge region. The observed Ag accumulation position is in accordance with Ref. [32].
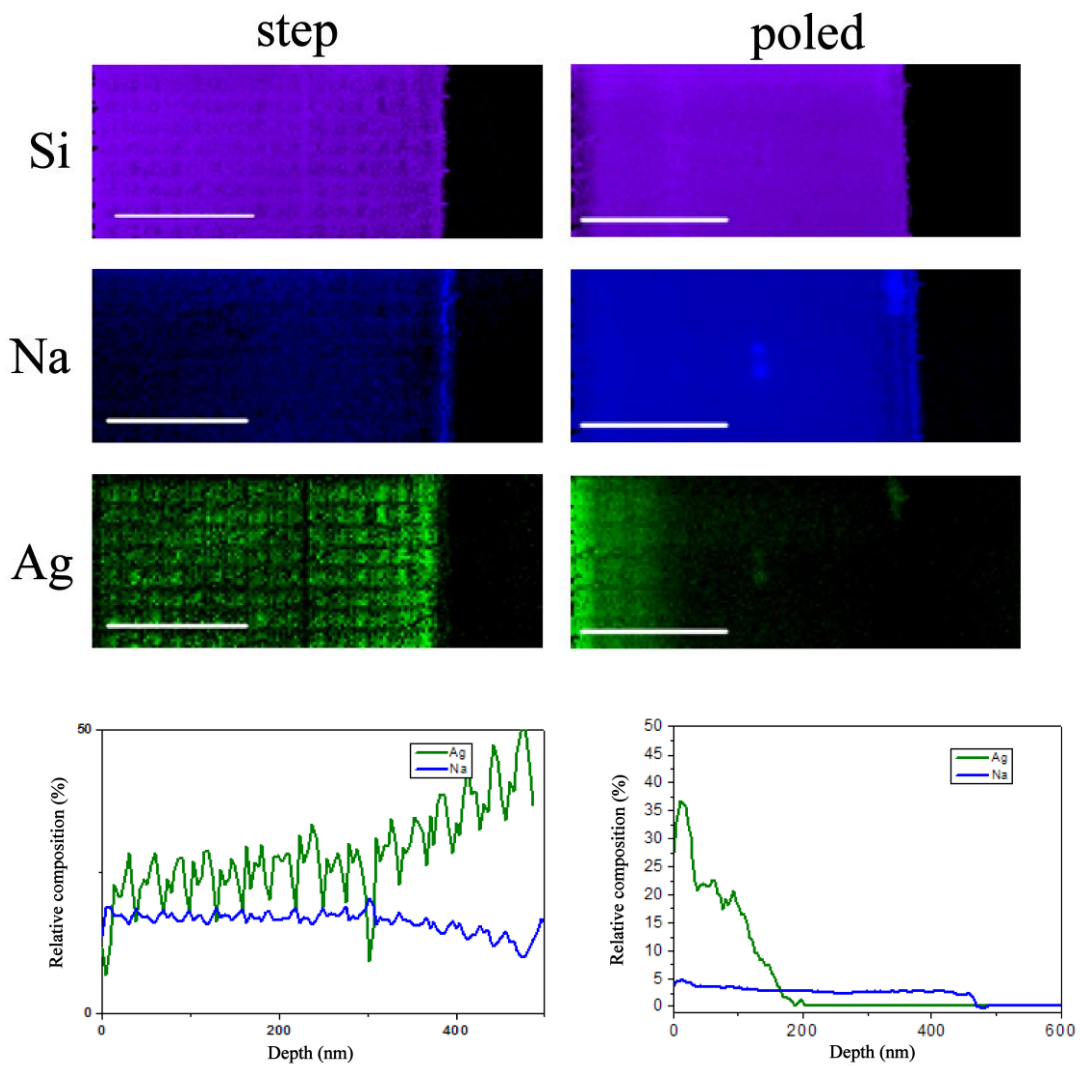

Fig. 13. Top panels: STEM-EELS composition maps for Na (blue), Si (violet) and Ag (green) for the step (left) and poled (right) samples. Scale bar corresponds to 200 nm. Bottom panels: subanodic region relative composition for the standard sample coated 45 min after poling. Coating was removed before the analysis.

Based on the presented results confirming that Ag^+ has diffused into glass without IE, conclusion is that its diffusion happens due to the absence of H^+/H_3O^+ to compensate the lack of positive charge in anodic surface sublayer. Charge compensation mechanism for poling in vacuum is the process of switching non-bridging oxygen bonds to bridging oxygen bonds with the release of O^-. However, this process is insufficient to compensate for all positive charge that drifted deeper into glass. For this reason uncompensated space charge remains in subanodic zone close to the surface after poling is finished [8]. Space charge intensity significantly reduces within hours upon exposure to the atmosphere [16]. Therefore, it is suggested that in the case of the sample kept in vacuum until coating, Ag^+ from the coating solution drifted into glass to compensate positive charge carriers in depleted zone and not due to IE. The subsurface layer of the other sample, kept at normal atmosphere for two days, compensated the lack of positive charge by cations from air and thus "closed" glass to Ag^+. It is clear that depletion of Na^+ due to GP, i.e., absence of IE, is not sufficient to explain higher concentration of Ag NPs in the coating over poled region alone. GP must be accompanied with H^+/H_3O^+ space charge compensation in subsurface zone in order to prevent Ag^+ diffusion into glass efficiently.

STEM-EELS results, obtained using Na K edge at 1072 eV (blue), Si K edge at 1839 eV (violet) and Ag M edge at 367 eV (green), indicate that the analysed air poled sample was coated sooner than the surface layer compensated for the positive charge, so some quantity of Ag^+ was able to diffuse into the glass. Nevertheless, this quantity seems to be negligible for optical properties as optical measurements for this sample do not significantly differ from the measurements of the sample coated 1 hour after poling (Fig.6). Results for the sample coated after one week may suggest that it is beneficial to leave substrate uncoated in the air more than 1 day. However, this result may be also a consequence of nonuniformity or some degree of spin coating unrepeatability.

GP set-up applied in this study, with anode pressed onto substrates surface, is so called semi opened poling mode. It enables H^+/H_3O^+ from air to enter into glass, but not in so high extent as in opened non-contact mode that enables alkalis with lower than sodium mobility, such as Ca^{2+} and Mg^{2+}, to remain close to the surface [33, 34]. In the work where selectively poled glass is immersed into hot Ag salt melt, the evidence of Ag NPs were found within poled glass as well [22]. Poling in that case was made with pressed nanostructured electrode consisting of stripes and grooves. As result, subsurface depletion region still contained Ca^{2+} and Mg^{2+}. These ions perhaps could participate in IE despite of their low mobility and charge.

Nevertheless, semi opened GP mode seems to be ideal for the purpose of preventing Ag^+ diffusion from the coating. Also, it is simple to realize this set up. Compared with opened non-contact mode, it has big advantage that by application of microstructured anode is the possibility of obtaining selectively poled and non-poled regions. However, it would be interesting to check the results of the opened non-contact mode treated sample as well.

4. Conclusions

It was demonstrated that GP increases the susceptibility for *in situ* formation of Ag and Au NPs by the reduction of a metal salt on alkali containing glasses. Six-fold increase in Ag plasmon ε_2 intensity was demonstrated after GP compared with virgin glass sample, the intensity high as in the case of quartz substrate. To achieve so high ε_2 values, it was not necessary to use chemical treatment for special cleaning or functionalization of glass surface. Comparing coatings on poled and plasma cleaned substrates, the first one presents more intense plasmon. Great advantage of pre-treatment with GP is that the effect does not change with long exposure to normal atmosphere, which means it is possible to prepare substrates much in advance before coating them. Also, there is no need for storing them in special conditions. The effect is not significantly affected by the presence of thin dielectric or Cr films. This fact broadens the applicability of GP as substrate surface pre-treatment method to multilayer systems as well. GP prevents unwanted IE between coating and glass by formation of subsurface zone depleted from alkalis. It is important that GP is followed by H^+/H_3O^+ space charge compensation in subsurface zone to prevent the unwanted compensation by metal ions from the coating. Semi opened GP applied in this study seems to be ideal for this purpose. It is simple to realize its set-up and it enables obtaining selectively poled regions by application of microstructured anode.

References

[1] U. Kreibig, M. Vollmer, Optical Properties of Metal Clusters, Springer, 1995.

[2] J.-N. Yih, W.-C. Hsu, S.-Y. Tsai, S.-J. Chen, Enhanced readout signal of superresolution near-field structure disks by control of the size and distribution of metal nanoclusters, Appl. Opt. 44 (2005) 3001. https://doi.org/10.1364/ao.44.003001.

[3] V. Janicki, J. Sancho-Parramon, H. Zorc, Gradient silver nanoparticle layers in absorbing coatings - experimental study, Appl. Opt. 50 (2011) C228. https://doi.org/10.1364/AO.50.00C228.

[4] V. Janicki, T.V. Amotchkina, J. Sancho-Parramon, H. Zorc, M.K. Trubetskov, A.V. Tikhonravov, Design and production of bicolour reflecting.coatings with Au metal island films, Opt. Exp. 19 (2011) 25521. https://doi.org/10.1364/OE.19.025521.

[5] H. Lyang, W. Wang, Y. Huang, S. Zhang, H. Wei, H. Xu, Controlled Synthesis of Uniform Silver Nanospheres, J. Phys. Chem. C 114 (2010) 7427. https://doi.org/10.1021/jp9105713.

[6] G. Lee, H. Lee, K. Nam, J.-H. Han, J. Y., S. W. L., D. S. Yoon, K. Eom, T. Kwon, Nanomechanical characterization of chemical interaction between gold nanoparticles and chemical functional groups, Nanoscale Res. Lett. 7 (2012) 608. https://doi.org/10.1186/1556-276X-7-608.

[7] P.-Y. Lin, G.-Y. Le, W.-I. Chiu, R.-Sh. Jian, Ch.-J. Lu, A single light spot GC detector employing localized surface plasmon resonance of porous Au@SiO2 nanoparticle multilayer, Analyst 144 (2019) 698. https://doi.org/10.1039/c8an01921e.

[8] M. Dussauze, V. Rodriguez, A. Lipovskii, M. Petrov, C. Smith, K. Richardson, T. Cardinal, E. Fargin, E.I. Kamitsos, How does thermal poling affect the structure of soda-lime glass?, J. Phys. Chem. C 114 (2010) 12754. https://doi.org/10.1021/jp1033905.

[9] J.E. Shelby, Introduction to Glass Science and Technology, Royal Society of Chemistry, 2015.

[10] A. V. Redkov, V. G. Melehin, A. A. Lipovskii, „How does thermal poling produce interstitial molecular oxygen in silicate glasses?" The J. Phys. Chem. C **119** 17298 (2015). https://doi.org/10.1021/acs.jpcc.5b04513.

[11] D. Yudistra, D. Faccio, C. Corbari, P. G. Kazansky, S. Benchabane, V. Pruneri, Electric surface potential and frozen-in field direct measurements in thermally poled silica, Appl. Phys. Lett. 92 (2008) 012912. https://doi.org/10.1063/1.2827175.

[12] R. Oven, Measurent of the refractive index of electrically poled soda-lime glass layers using leaky modes, Appl. Opt. 55 (2016) 9123. https://doi.org/10.1364/AO.55.009123.

[13] M. Dussauze, E.I. Kamistos, E. Fargin, V. Rodriguez, Refactive index distribution in the non-linear optical layer of thermally poled oxide glasses, Chem. Phys. Lett. 470 (2009) 63. https://doi.org/10.1016/j.cplett.2009.01.007.

[14] I. Fabijanić, P. Pervan, B. Okorn, J. Sancho-Parramon, V. Janicki, Ellipsometry-based study of glass refractive index depth profiles obtained by applying different poling conditions, Appl. Opt. 59 (2020) A69. https://doi.org/10.1364/AO.59.000A69.

[15] A.A. Lipovskii, M. Kuittinen, P. Karvinen, K. Leinonen, V.G. Melehin, V.V. Zhurikhina, Yu.P. Svirko, Electric field imprinting of sub-micron patterns in glass-metal nanocomposites, Nanotechnology 19 (2008) 415304. https://doi.org/10.1088/0957-4484/19/41/415304.

[16] A. Lepicard, T. Cardinal, E. Fargin, F. Adamietz, V. Rodriguez, K. Richardson, M. Dussauze, „Surface reactivity control of a borosilicate glass using thermal poling," The J. Phys. Chem. C 119 22999 (2015). https://doi.org/10.1021/acs.jpcc.5b07139.

[17] A. Lepicard, T. Cardinal, E. Fargin, F. Adamietz, V. Rodriguez, K. Richardson, M. Dussauze, Micro-structuring the surface reactivity of a borosilicate glass via thermal poling, Chem. Phys. Lett. 664 (2016) 10. https://doi.org/10.1016/j.cplett.2016.09.077.

[18] E. Ziemath, V. Araujo, C. Escanhoela Jr, Compositional and structural changes at the anodic surface of thermally poled soda-lime float glass, J. Appl. Phys. 104 (2008) 054912. https://doi.org/10.1063/1.2975996.

[19] F. Lind, D. Palles, D. Moncke, E. Kamitsos, L. Wondraczek, Modifying the surface wetting behavior of soda-lime silicate glass substrates through thermal poling, J. Non-Crystalline Solids 462 (2017) 47. https://doi.org/10.1016/j.jnoncrysol.2017.02.006.

[20] A.V. Redkov, V.G. Melehin, D.V. Raskhodchikov, I.V. Reshetov, D.K. Tagantsev, V.V.Zhurikhina, A.A. Lipovskii, Modifications of poled silicate glasses under heat treatment, J. Non-Cryst.Sol. 503–504 (2019) 279. https://doi.org/10.1016/j.jnoncrysol.2018.10.011.

[21] E.S. Babich, E.S. Gangrskaia, I.V. Reduto, J. Béal, A.V. Redkov, T. Maurer, A.A. Lipovskii, Self-assembled silver nanoparticles in glass microstructured by poling for SERS application, Curr Appl. Phys. 19 (2019) 1088. https://doi.org/10.1016/j.cap.2019.07.003.

[22] E. Babich, I. Reduto, A. Redkov, I. Reshetova, V. Zhurikhina, A. Lipovskii, Thermal poling of glass to fabricate masks for ion exchange, J. Phys. Conf. Ser. 1695 (2020) 012107. https://doi.org/10.1088/1742-6596/1695/1/012107.

[23] T. Selvam, I. Fabijanić, Jordi Sancho-Parramon, Petar Pervan, V. Janicki, Optical microstructures based on surface-selective growth of Ag nanoparticles on thermally poled soda-lime glass, in press in Optics Letters.

[24] J. Sancho-Parramon, V. Janicki, H. Zorc, Tuning the effective dielectric function of thin film metal-dielectric composites by controlling the deposition temperature, J. Nanophotonics 5 (2011) 051805. https://doi.org/10.1117/1.3590238.

[25] C.F. Bohren, D.R. Huffman, Absorption and Scattering of Light by Small Particles, John Wiley & Sons, 2008.

[26] Y. Yang, P. Zhou, Sh.-X. Zhang, X.-G. Guo, D.-M. Guo, Effect of substrate curvature on thickness distribution of polydimethylsiloxane thin film in spin coating process, Chyn. Phys. B 27 (2018) 068104. https://doi.org/10.1088/1674-1056/27/6/068104.

[27] H.K. Pulker, Coatings on Glass, first ed., Elsevier Science, 1987.

[28] Y. Chimupala, G. Hyett, R. Simpson, R. Mitchell, R. Douthwaite, S.J. Milne, R.D. Brydson, Synthesis and characterization of mixed phase anatase TiO_2 and sodium-doped $TiO_2(B)$ thin films by low pressure chemical vapour deposition (LPCVD), RSC Adv. 4 (2014) 48507. https://doi.org/10.1039/c4ra07570f.

[29] E. Aubry, J. Lambert, V. Demange, A. Billard, Effect of Na diffusion from glass substrate on the microstructural and photocatalytic properties of post-annealed TiO_2 films synthesised by reactive sputtering, Surf. Coat. Technol. 206 (2012) 4999. https://doi.org/10.1016/j.surfcoat.2012.06.012.

[30] E. Cataruzza, F. Gonella, Sh. Ali, V. Bello, T, Cesca, A solid-state route for the synthesis of metal nanocluster composite glasses, Solid State Phenom. 151 (2009) 252. https://doi.org/10.4028/www.scientific.net/SSP.151.252.

[31] C.M. Lepienski, J.A. Giacometti, G.F. Leal Ferreira, F.L. Freire Jr., C.A. Achete, Electric field distribution and near-surface modifications in soda-lime glass submitted to a dc potential, J. Non-Cryst. Sol. 159 (1993) 204. https://doi.org/10.1016/0022-3093(93)90224-L.

[32] E. Babich, E. Lubyankina, V. Kaasik, V. Mozharov, I. Mukhin, V. Zhurikhina, A. Lipovskii, Visualization of spatial charge in thermally poled glass via nanoparticles formation, Nanomaterials 11 (2021) 2973. https://doi.org/10.3390/nano11112973.

[33] M. Chazot, M. Paraillous,S. Jouannigot, L. Teulé-Gay, J.-P. Salvetat, F. Adamietz, R. Alvardo-Meza, L. Karam, A. Poulon, T. Cardinal, E. Fargin, M. Dussauze, Enhancement of mechanical properties and mechanical durability of soda-lime silicate glasses treated by DC gas discharges, J. Am. Cerac. Soc. 104 (2021) 157. https://doi.org/10.1111/jace.17438.

[34] A. Degarchev, V. Kaasik, A. Lipovskii, V. Melehin, A. Redkov, I. Reshetov, D. Taganatsev, Control of soda-lime glass surface crystallization with thermal poling, J. Non.-Cryst. Sol. 533 (2020) 119899. https://doi.org/10.1016/j.jnoncrysol.2020.119899.